DETECTING DYNAMIC AND GENETIC EFFECTS ON BRAIN STRUCTURE USING HIGH-DIMENSIONAL CORTICAL PATTERN MATCHING

Paul M. Thompson[1], Kiralee M. Hayashi[1], Greig de Zubicaray[2], Andrew L. Janke[2,3], Stephen E. Rose[2], James Semple[4], David M. Doddrell[2], Tyrone D. Cannon[1], Arthur W. Toga[1]

[1]Laboratory of Neuro Imaging, UCLA School of Medicine, Los Angeles; [2]Centre for Magnetic Resonance, Univ. of Queensland, Australia; [3]McConnell Brain Imaging Center, Montreal Neurological Institute, McGill University, Canada; [4]GlaxoSmithKline Pharmaceuticals plc, Cambridge, UK

ABSTRACT

We briefly describe a set of algorithms to detect and visualize effects of disease and genetic factors on the brain. Extreme variations in cortical anatomy, even among normal subjects, complicate the detection and mapping of systematic effects on brain structure in human populations. We tackle this problem in two stages. First, we develop a cortical pattern matching approach, based on metrically covariant partial differential equations (PDEs), to associate corresponding regions of cortex in an MRI brain image database (*N*=102 scans). Second, these high-dimensional deformation maps are used to transfer within-subject cortical signals, including measures of gray matter distribution, shape asymmetries, and degenerative rates, to a common anatomic template for statistical analysis. We illustrate these techniques in two applications: (1) mapping dynamic patterns of gray matter loss in longitudinally scanned Alzheimer's disease patients; and (2) mapping genetic influences on brain structure. We extend statistics used widely in behavioral genetics to cortical manifolds. Specifically, we introduce methods based on h-squared distributed random fields to map hereditary influences on brain structure in human populations.

1. INTRODUCTION

Computational brain atlases, which represent anatomy in a standardized 3D coordinate system, show enormous promise in detecting systematic patterns of brain structure and function in human populations. These atlases are empowered by recent algorithmic advances in computational anatomy ([1]; see [2] for a recent review). Combining concepts from differential geometry, continuum mechanics, computer vision and shape modeling, these methods can identify disease effects on the brain, how these patterns progress dynamically over time, and how drug treatment, age, gender, risk genes or environmental influences modulate them. Population-based atlases in particular [3] can synthesize multi-modality brain imaging data from patients with Alzheimer's disease (AD) [4,5], schizophrenia [6], twins [7], and developing children [8], often identifying key patterns of development and disease that are not apparent in an individual subject.

Cortical anatomy is so complex and variable that it is difficult to compare and integrate brain data in human populations. To assist in pooling cortical data across subjects, some methods first unfold a computational model of the cortex to a spherical shape or 2D plane. Features are then matched using a nonlinear flow in the resulting 2D parameter space. This flow can be represented by spherical harmonics [9,10], which are eigenfunctions of the spherical Laplacian, or by solving an elastic or fluid PDE that aligns sulcal/gyral landmarks [11,12] or curvature maps [13]. We describe an approach, based on covariant PDEs, which makes these flows invariant to the way the cortical surfaces are parameterized. When the self-adjoint differential operator governing the PDE is discretized, fields of Christoffel symbols are derived from the metric tensor of the surface domain and added as correction terms. The matching fields are then independent of the surface metrics, and can be used to associate signals from corresponding cortical regions across subjects. We show illustrative applications of the approach in Alzheimer's disease and genetics.

2. METHODS

Imaging and Subject Populations. 3D MRI (SPGR) scans were acquired longitudinally (interscan interval 2.6±0.3 yrs.) from 17 AD patients and 14 healthy control subjects matched for age, sex, and handedness (final age: 71.3±1.8 yrs.). An additional 40 3D MRI scans were acquired from 20 pairs of healthy twins (10 identical or monozygotic (MZ) pairs, 10 fraternal or dizygotic (DZ)) matched for age (48.2±3.4 years), sex, and handedness. After affine alignment of individual data to a group average size and shape [4], gyral pattern and shape variations were encoded using high-dimensional elastic deformation mappings (see Figs. 1,2) driving each subject's cortical anatomy into a group average configuration.

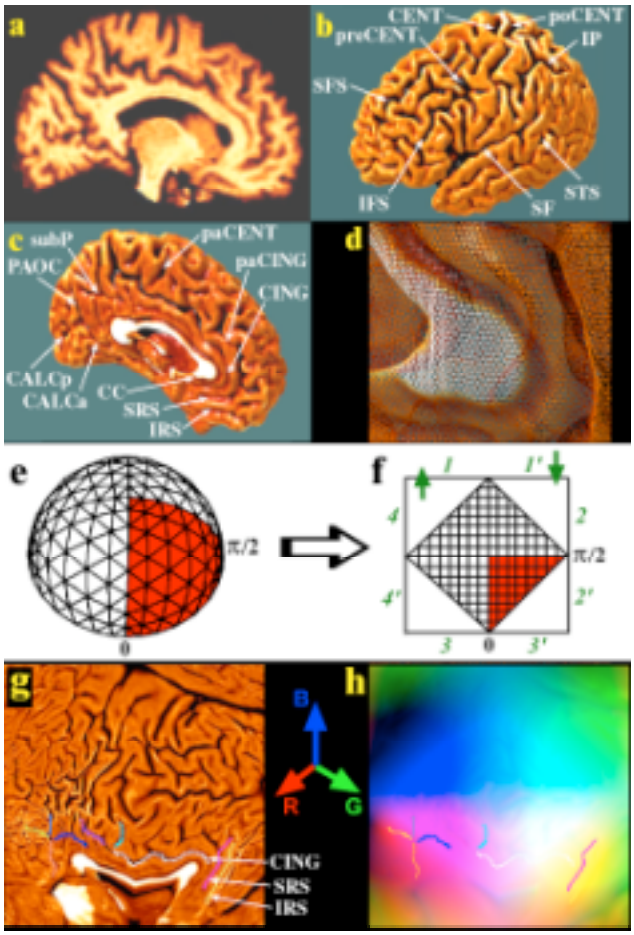

Figure 1: *Cortical Gridding*. Cortical models are created from each 3D MRI scan (a) by driving a tiled, spherical mesh into the configuration of each subject's cortex; one sphere represents each hemisphere (b) [14]. 36 uniform speed parametric 3D curves per hemisphere (c) are manually identified representing all consistently appearing gyral/sulcal landmarks. Each cortical hemisphere i is parameterized (d) with an invertible mapping D_i: $(\theta,\phi) \mapsto$ (x,y,z), so sulcal curves and landmarks in the folded brain surface can be reidentified in a spherical map (e). To facilitate the discretization of PDEs on the surface, spherical coordinates (e) are replaced by a flat square 2D multigrid structure (of side π; (e)). In this data structure, no cuts are introduced: connectivity information is retained between boundary nodes that are adjacent on the 3D brain surface (e.g. 1 matches 1', 2 matches 2', etc.). Green arrows denote points that are topographically adjacent. In this scheme, cortical points with spherical coordinates (θ,ϕ) lying in the octant $[0,\pi/2]\times[0,\pi/2]$ (*colored red*, (e)), map to the 2D parameter space location $(\theta,\phi(\pi-2\theta)/\pi)$ (*red triangle*, (f)). Other mappings are then determined by symmetry. To retain relevant 3D information when flattening the cortex (g), cortical surface point position vectors (x,y,z) in 3D stereotaxic space are color-coded via a linear look-up table using a unique RGB color triplet. This forms an image of the parameter space in color image format (h).

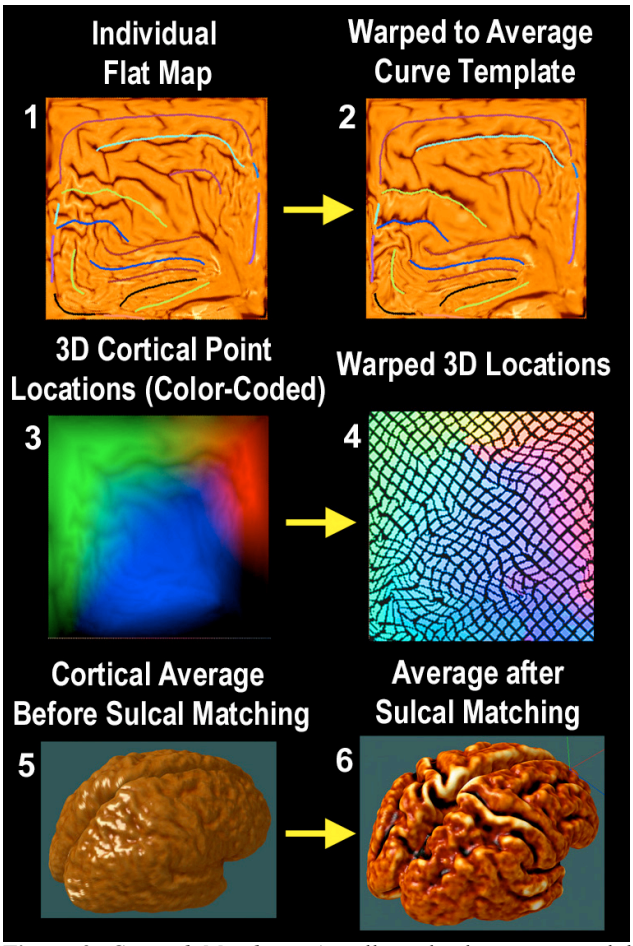

Figure 2: *Cortical Matching*. A well-resolved average model of the cerebral cortex (6) can be built for any group of subjects. (1) shows a magnified region of the 2D cortical parameter space for a particular subject, and its corresponding color code (3). These are both warped (2,4) to match an average set of sulcal curves in parameter space. If the warped color images (4) are averaged pixel-by-pixel across subjects, they can be decoded to produce a crisp average model of the cortex (6). The internal alignment of landmarks is necessary to avoid destructive cancellation of features (5). This cancellation would also happen if images were averaged together directly in stereotaxic space. Common features are reinforced in the group average and appear in their group mean anatomical locations. Cortical measures such as gray matter density are then subsequently convected along with these flows and plotted on the average cortex, prior to statistical analysis (Fig. 3).

Cortical Matching. Cortical differences between any pair of subjects were calculated as follows. A flow field is first calculated that elastically warps each flat map (Fig. 2(1)) onto an average set of sulcal curves in parameter space (Fig. 2(2)). On the sphere, the parameter shift function $\mathbf{u}(\mathbf{r})$: $\Omega \mapsto \Omega$, is given by the solution F: $\mathbf{r} \mapsto \mathbf{r}-\mathbf{u}(\mathbf{r})$ to a curve-driven warp in the spherical parametric space $\Omega=[0,2\pi)\times[0,\pi)$. For points $\mathbf{r}=(r,s)$ in the parameter space (Fig. 1(d)), a system of simultaneous partial differential equations is written for the flow field $\mathbf{u}(\mathbf{r})$:

$$L^{\ddagger}(\mathbf{u(r)}) + \mathbf{F(r-u(r))} = \mathbf{0}, \ \mathbf{r} \in \Omega, \text{ with } \mathbf{u(r)} = \mathbf{u_0(r)}, \ \mathbf{r} \in M_0 \cup M_1. \quad (1)$$

Here M_0, M_1 are sets of points and (sulcal or gyral) curves where displacement vectors $\mathbf{u(r)}=\mathbf{u_0(r)}$ matching corresponding anatomy across subjects are known. The flow behavior is modeled using continuum-mechanical equations. L can be any second order self-adjoint differential operator; here we use the Cauchy-Navier differential operator $L = \mu\nabla^2+(\mu+\lambda)\nabla(\nabla^T\bullet)$ with body force $\mathbf{F}$ (*cf.* [15,16]). To create mappings that are independent of the surface metrics (parameterizations), we use $L^{\ddagger}$, the *covariant* form of the differential operator L. $L^{\ddagger}$, all L's partial derivatives are replaced with *covariant* derivatives with respect to the metric tensor of the surface domain where calculations are performed. The covariant derivative of a (contravariant) vector field, $u^i(\mathbf{x})$, is: $u^i_{,k} = \partial u^i/\partial x^k + \Gamma^j_{ik}\, u^i$ where the *Christoffel symbols of the second kind*, Γ^j_{ik}, are computed from derivatives of the metric tensor components $g_{jk}(\mathbf{x})$:

$$\Gamma^i_{jk} = (1/2)\, g^{il}\, (\partial g_{lj}/\partial x^k+\partial g_{lk}/\partial x^j-\partial g_{jk}/\partial x^i). \quad (2)$$

These correction terms are then used in the solution of PDE, producing a family of 3D deformation maps, $\mathbf{U}_i(\mathbf{r})$ matching each individual cortex in 3D to the average cortex for a group. Here $\mathbf{U}_i$ is a 3D location on the *i*th subject's cortex, and $\mathbf{r}$ is the location it maps to, after warping, in the cortical parameter space.

Mapping Gray Matter Deficits. All MRIs were RF-corrected and segmented with a Gaussian mixture classifier, producing binary maps of gray matter. Let $g_{i,r}(\mathbf{x})$ be the '*gray matter density*', i.e. the proportion of voxels classified as gray matter falling within a sphere (center $\mathbf{x}$, radius $\mathbf{r}$) in the *i*th subject's scan. Then for a point at parameter location $\mathbf{r}$ on the group average cortex (Fig. 2(6)), $g_{i,r}(\mathbf{U}_i(\mathbf{r}))$ is the gray matter density at the corresponding cortical point in subject *i*.

3. RESULTS

After averaging the aligned maps of gray matter density across groups of patients with Alzheimer's disease and healthy controls, Fig. 3 reveals the spatial profile of gray matter deficits in disease. By averaging the aligned maps, and texturing them back onto a group average model of the cortex, the average magnitude of gray matter loss was computed for the Alzheimer's disease population (Fig. 3; (*cf.* [17]). Regions with up to 10-20% reduction in the measure are demarcated from adjacent regions with little detectable loss. The group effect size was measured by attaching a field of *t* statistics, $t(\mathbf{r})$, to the cortical parameter space, and computing the area of the *t* field on the group average cortex above a fixed threshold ($p < 0.01$, uncorrected). In a multiple comparisons correction, the significance of the overall effect was confirmed to be $p < 0.01$, by permuting the assignment of subjects to groups 1,000,000 times.

Genetic Effects. In a second application, the intraclass correlation in gray matter distribution $g_{i,r}(\mathbf{x})$ was computed for groups of identical and fraternal twins, after cortical pattern matching (giving maps $r_{MZ}(\mathbf{r},\mathbf{r})$ and $r_{DZ}(\mathbf{r},\mathbf{r})$ in Fig. 4). In behavioral genetics, a feature is *heritable* if r_{MZ} significantly exceeds r_{DZ}. An estimate of its heritability h^2 can be defined as $2(r_{MZ}-r_{DZ})$, with standard error: $\text{S.E.}^2(h^2)=4[((1-r_{MZ}^2)^2/n_{MZ}) + ((1-r_{DZ}^2)^2/n_{DZ})]$. In Fig. 4, we computed a *heritability map* from the equation:

$$h^2(\mathbf{r},\mathbf{r})=2(r_{MZ}(\mathbf{r},\mathbf{r})-r_{DZ}(\mathbf{r},\mathbf{r})).$$

Strong genetic influences on frontal brain structure were visualized. These effects were confirmed by assessing the significance of effect size of h^2 by permutation (this involved repeated generation of null realizations of an h^2-distributed random field; see Fig. 4; see details in [18]).

4. CONCLUSION

Algorithms to map disease-related and genetic effects on the cortex can reveal key features of brain development and degeneration. We described a cortical pattern matching approach to assist in normalizing signals on the cortex. We used this to map degenerative profiles in Alzheimer's disease, taking into account the wide variations in gyral patterning. Finally, we developed a method to isolate genetic effects on cortex. We extended statistics used widely in behavioral genetics to a brain mapping application. These maps will be key components of future disease-specific and genetic brain atlases.

Supported by grants P41 RR13642, LM/MH05639, NINDS/NIMH NS38753, P20 MH/DA52176.

4. REFERENCES

[1]. Miller MI et al. (2002). On the Metrics and Euler-Lagrange Equations of Computational Anatomy [in press].

[2]. Thompson PM, Toga AW (2002). *A Framework for Computational Anatomy*, Comp. Vis. in Science 5:1-12.

[3]. Mazziotta JC et al. (2001). *A Probabilistic Atlas and Reference System for the Human Brain,* J. Royal Soc. 356(1412):1293-1322.

[4]. Thompson PM et al. (2000). *Mathematical/ Computational Challenges in Creating Population-Based Brain Atlases*, Human Brain Mapping 9(2):81-92

[5]. Janke AL, Zubicaray Gd, Rose SE, Griffin M, Chalk JB, Galloway GJ (2001). *4D deformation modeling of cortical disease progression in Alzheimer's dementia*. Magn. Reson. Med. 46(4):661-6.

[6]. Thompson PM et al. (2001). *Mapping Adolescent Brain Change Reveals Dynamic Wave of Accelerated Gray Matter Loss in Very Early-Onset Schizophrenia*, Proc. Nat. Acad. Sci. USA 98(20):11650-11655.

[7]. Cannon TD, Thompson PM et al. (2001). *Cortex Mapping Reveals Regionally Specific Patterns of Genetic and Disease-Specific Gray Matter Deficits in Twins Discordant for*

Schizophrenia, Proc. Nat. Acad. Sci. USA 99(5):3228-3233.
[8]. Thompson PM et al. (2000). *Growth Patterns in the Developing Brain Detected By Using Continuum-Mechanical Tensor Maps*, Nature 404(6774):190-193.
[9]. Thompson PM, Toga AW (1996). *A Surface-Based Technique for Warping 3-Dimensional Images of the Brain*, IEEE Transactions on Medical Imaging 15(4):1-16.
[10]. Gerig G et al. (2001). *Shape versus Size: Improved Understanding of the Morphology of Brain Structures*, Proc. MICCAI 2001, Springer LNCS 2208:24-32.
[11]. Davatzikos C et al. (2001). *Voxel-based morphometry using the RAVENS maps: methods and validation using simulated longitudinal atrophy.* Neuroimage 14(6):1361-9.
[12]. Bakircioglu M et al. (1999). *Landmark Matching on Brain Surfaces via Large Deformation Diffeomorphisms on the Sphere*, Proc. SPIE Medical Imaging 1999.
[13]. Fischl B et al. (1999). *High-Resolution Inter-Subject Averaging and a Coordinate System for the Cortical Surface*, Hum Brain Mapp. 8(4):272-84.
[14]. MacDonald D (1998). *A Method for Identifying Geometrically Simple Surfaces from Three Dimensional Images*, PhD Thesis, McGill Univ., Canada.
[15]. Gee JC, Bajcsy RK (1998). *Elastic Matching: Continuum-Mechanical and Probabilistic Analysis*, in: Toga AW [ed.], Brain Warping, Academic Press, San Diego.
[16]. Christensen GE et al. (1996). *Deformable Templates using Large Deformation Kinematics*, IEEE TMI 5(10):1435-1447.
[17]. Studholme C et al. (2001). *Detecting Spatially Consistent Structural Differences in Alzheimer's and Fronto-temporal Dementia Using Deformation Morphometry*. MICCAI: 41-48.
[18]. Thompson PM, Cannon TD et al. (2001). *Genetic Influences on Brain Structure,* Nature Neuroscience 4(12):1253-8.

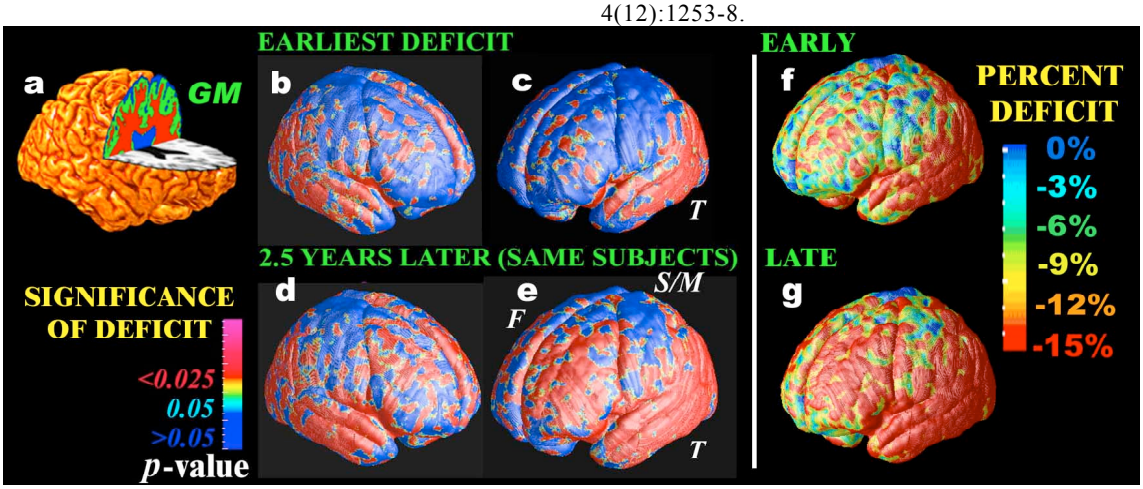

Figure 3: *Mapping Gray Matter Deficits in Alzheimer's Disease.* Here cortical pattern matching was used to associate measures of gray matter density from corresponding cortical regions, in 3D MRI scans (a) of 17 AD patients and 14 matched controls. Temporal brain regions exhibit significant gray matter (GM) deficits in both brain hemispheres (*red colors*: (b),(c)). The experiment was repeated based on an independent set of scans of all the same subjects acquired 2.5 years later. By this time the patients' MMSE cognitive test scores has deteriorated from a score of 17.7±6.2 to 12.9±8.2 (mean±SD). Notice how tissue losses had intensified [(d),(e)] from 5-10% initially (f) to a 15% gray matter deficit (g) in frontal cortices.

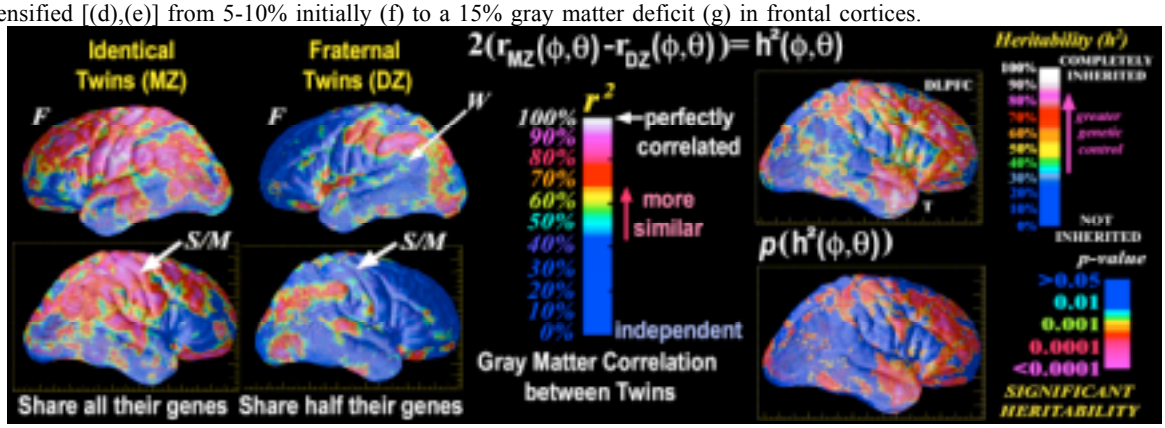

Figure 4. *Mapping Genetic Influences on Brain Structure*. Once gray matter maps are aligned across subjects, using cortical pattern matching, intrapair individual differences can be compared for identical twins (MZ; *left panels*) who share all their genes, and fraternal twins (DZ), who on average share half. The intraclass correlation in gray matter density is higher for MZ than DZ twins. A plot of twice their difference (*top right*) shows high heritability values $h^2(\phi,\theta)$ in dorsolateral prefrontal cortex (DLPFC). The significance of these genetic influences on brain structure was confirmed by thresholding the experimental significance map $p(h^2(\phi,\theta))$ and comparing its supra-threshold extent with simulated realizations of h^2-distributed random fields (see [18]).